Backward magnetostatic surface spin waves in coupled Co/FeNi bilayers

Wenjie Song[†,1], Xiansi Wang[†,2], Wenfeng Wang[1], Changjun Jiang[1], Xiangrong Wang[*,3,4], Guozhi Chai[*,1],

[1] Key Laboratory for Magnetism and Magnetic Materials of the Ministry of Education, Lanzhou University, Lanzhou, 730000, People's Republic of China
[2] Center for Quantum Spintronics, Department of Physics, Norwegian University of Science and Technology, NO-7491 Trondheim, Norway
[3] Department of Physics, The Hong Kong University of Science and Technology, Clear Water Bay, Kowloon, Hong Kong, People's Republic of China
[4] HKUST Shenzhen Research Institute, Shenzhen 518057, People's Republic of China

Key words: Backward surface spin waves, Brillouin light scattering, negative group velocities

[*] Corresponding author: e-mail phxwan@ust.hk chaigzh@lzu.edu.cn
† These authors contributed equally to this work.

Spin waves in coupled Co/FeNi bilayers are probed by Brillouin light scattering technique. Two types of spin waves, magnetostatic surface spin waves and perpendicular standing spin waves, were identified. The dispersion relations of magnetostatic surface spin waves obtained from the Stokes and anti-Stokes measurements display respectively positive and negative group velocities. The anti-Stokes branch with positive phase velocities and negative group velocities is called backward magnetostatic surface mode that originates from the magnetostatic interaction in the bilayer. Experimental data agree well with our theoretical calculations. Our results can be used to understand spin waves propagation.

Copyright line will be provided by the publisher

Spin waves (SWs) in magnetic films have attracted much attention in recent years because of great potential applications in spintronic devices.[1–7] SWs are collective oscillations of spins at gigahertz frequency in typical ferromagnetic materials.[8,9] Their wavelengths are of orders of magnitude shorter than that of electromagnetic waves at the same frequency so that SWs can be used in micro or nano size spin wave devices.[2,3,8–10] SWs can be classified by the dominating interactions as exchange type and magnetostatic one.[11,12] It is well-known that there are three different kinds of magnetostatic SWs in thin ferromagnetic films. They are the magnetostatic surface spin waves (MSSWs) that are also known as the Damon-Eshbach (DE) mode, the backward volume magnetostatic spin waves (BVMSWs) and the forward volume magnetostatic spin waves (FVMSWs).[3,13–16] The MSSWs are nonreciprocal and exhibit different characteristics at different interfaces of magnetic films.[3,14] For both MSSWs and FVMSWs, the slope of the dispersion relations are positive for positive frequencies and wavevectors so that both of phase and group velocities are positive, but not equal in general.[3,14] The BVMSWs has positive phase velocities and negative group velocities. This backward propagation is useful in velocity-related applications such as the inverse Doppler effect.[3,17,18] One interesting question is whether a negative group velocity can happen to MSSWs in a hybridized system. Such backward MSSWs should be very interesting and important because surface SWs are in general useful in SW-based devices such as SW filters, SW beamspliters, and SW emitters.[1,19–27]

Conventional nonreciprocal MSSWs are unidirectional and propagate along $\mathbf{m} \times \mathbf{n}$. Here $\mathbf{m}$ is the magnetization direction and $\mathbf{n}$ is the normal direction of the surface that points outward of the magnetic film. Thus $\mathbf{n}$ is up for the upper surface and down for the bottom surface.[13] When two magnetic layers are stacked together, there are pairs of left- and right-propagating waves localized at the top and bottom surfaces of two layers. The two

Copyright line will be provided by the publisher

counter-propagating waves are strongly coupled. As shown by previous works on very thin bilayers, this coupling can induce non-reciprocity for the interface MSSWs,[28–32] yet still with positive group velocities. Recently, there are indications of backward MSSW in YIG/YIG/GaAs multilayers.[33] However, only few data points with very long wavelength (k<5 rad/μm) were provided, probably due to small saturation magnetization of YIG as well as the similarity of two YIG layers. According to the previous theoretical studies [29], we expect that backward MSSWs are possible when two counter-propagating MSSWs are sufficiently different from each other (can be realized in materials with very different saturation magnetization) and their coupling are strong enough. The reason that backward MSSWs were not found before is either because the film thickness is too small so that the coupling of MSSWs on different surfaces is important or because two MSSWs are too similar. Thus, we use thicker bilayers (Co/FeNi) in this study. Besides the usual nonreciprocal property of MSSWs from the magnetostatic interactions, the Dzyaloshinskii-Moriya interaction (DMI) is chiral in nature and can also lead to asymmetric dispersion relation that, in turn, results in nonreciprocal behavior of SWs.[34–36] In this letter, we use Brillouin light scattering (BLS) to obtain dispersion relations of surface SWs of Co/FeNi bilayer system. These two materials are chosen because of their distinct saturation magnetizations and other magnetic properties. The MSSWs and perpendicular standing spin waves (PSSWs) were observed. The dispersion relation of MSSWs obtained from the anti-Stokes measurements are backward MSSWs while that obtained from Stokes measurements has the usual MSSW spectrum. The experimental results agree well with the numerical calculations when true material parameters are used.

Our Co(30)/FeNi(t) bilayer films were deposited on single-crystal Si (111) substrates by radio frequency (RF) magnetron sputtering. The numbers in parentheses are the film thicknesses in nanometers. The FeNi layer thickness t varied from 30 to 50 nm that was controlled by varying the sputtering time (with 10% uncertainty in thickness). The base pressure of sputtering chamber was about 5×10^{-5} Pa. The pressure inside the chamber was 0.3 Pa and the RF power was 50 W during sputtering process. Static magnetization of Co(30)/FeNi(t) bilayer were measured by a vibrating sample magnetometer (VSM). Figure 1 shows the in-plane magnetic hysteresis loops of bilayer samples at room temperature when the field is applied along the easy magnetization axis (a) and along the hard magnetization axis (b). As shown in Fig. 1, the magnetic hysteresis loops are smooth in both cases. This means that the bilayer are coupled like a single layer.[37] FMR measurements and relevant experimental parameters can be found in supplementary materials.

BLS measurements were performed for the Co/FeNi bilayer at room temperature. Wavenumber-selective BLS is very effective in obtaining the dispersion relation of

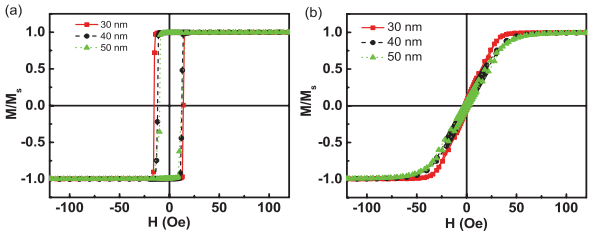

Figure 1 The normalized in-plane hysteresis loops of Co/FeNi bilayer. (a) The hysteresis loops of FeNi layer of various thicknesses. The field is along the easy magnetization axis. (b) The hysteresis loops of FeNi layer of various thicknesses. The field is along the hard magnetization axis.

surface waves.[38–40] The scattering process can be described by inelastic scattering and is known as the 180° backscattering geometry (see inset of Fig. 2(a)). In experiments, external magnetic field **H** is in-plane and perpendicular to the MSSWs wave vector. The incident plane of the laser light is perpendicular to the external field as shown in the inset of Fig. 2(a). The wave vector of the MSSWs is $k_{\|} = 4\pi \sin\theta/\lambda$, where the θ is the incident angle of the light and λ is laser wavelength (532 nm). The laser power incident on the surface of the sample is about 30 mW in the experiments.[34,41] In our work, the range of $k_{\|}$ varies from -16.53 rad/μm to 16.53 rad/μm with a step size of 1.18 rad/μm by varying the laser light incident angle. In our experiment, the distance between the mirrors is 5 mm. Free spectral range of the interferometer is $\pm$34.94 GHz along with 1024 channels in the ADC. The resolution of the scanning frequency is 0.068 GHz. The typical BLS spectra for FeNi(30) single layer and Co(30)/FeNi(30) bilayer are illustrated in Fig. 2 with the absolute value of wave vector $k_{\|}$ = 16.53 rad/μm and external magnetic field **H** = 500 Oe. In the light scattering process, the wave-vector change in the anti-Stokes scatterings (positive frequency) is defined as the positive and that in the Stokes scatterings (negative frequency) is defined as the negative. From Fig. 2, both the FeNi(30) single layer and the Co(30)/FeNi(30) bilayer spectrum display four different peaks. The two peaks of larger signal are for MSSWs and the other two peaks with weaker signal are for PSSWs. For the FeNi(30) single layer, the MSSWs show one Stokes peak $f(-k)$ with a negative frequency shift (-12.87 GHz) and one anti-Stokes peak $f(k)$ with positive frequency shift (12.82 GHz). This suggests that the two MSSWs propagate in opposite directions and with the same absolute value of frequency within experimental error. However, for the Co(30)/FeNi(30) bilayer, the MSSWs of Co(30)/FeNi(30) bilayer show one Stokes peak $f(-k)$ with a negative frequency shift (-13.28 GHz) and one anti-Stokes peak $f(k)$ with positive frequency shift (9.67 GHz). This suggests that the two MSSWs propagate in opposite directions and have a distinct frequency difference. In contrast, for the PSSWs mode, the frequency of both FeNi(30)

Copyright line will be provided by the publisher

single layer and Co(30)/FeNi(30) bilayer are almost the same.

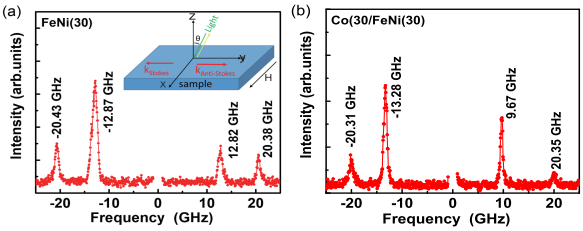

Figure 2 BLS spectrum measured for (a) FeNi(30) single layer and (b) Co (30)/FeNi(30) bilayer with the absolute value of wave vector $k_{\|}$ = 16.53 rad/μm and external magnetic field **H** = 500 Oe. Inset: Schematic of the scattering process of 180° backscattering geometry. The incident angle is denoted by θ. Magnetic field H is along the x-direction.

The dispersion relation of FeNi(30) single layer and Co(30)/FeNi(t) bilayers with various FeNi thicknesses of t = 30, 40, and 50 nm was measured by BLS. Figure 3 is the density plot of BLS intensity in frequency - wave vector plane. The left side of the vertical black dotted line correspond to negative wave vector (Stokes) and the right side of the vertical black dotted line correspond to positive wave vector (anti-Stokes). In the experiments, a constant magnetic of **H** = 500 Oe is along the x-direction and the $k_{\|}$ varies from -16.53 rad/μm to 16.53 rad/μm along the y-direction. As shown in Fig. 3(a), the lower frequency mode is MSSWs and higher frequency mode is PSSWs. For lower frequency mode, the frequency increases with the wave vector. For higher frequency mode, the frequency does not change with the wave vector. As shown in Fig. 3(b),(c),(d), the lower frequency mode of the Co(30)/FeNi(t) bilayers is MSSWs from the FeNi layer (no signal from Co due to the penetration depth of the laser light). The higher frequency mode is a mixture of PSSW and MSSW, dominated by PSSW (pure PSSW modes are drawn in white dashed line). For lower frequency mode, the $f(k-)$ increases with the increase of wave vector k, which behaves like the common MSSWs. However, the $f(k+)$ decreases with the increase of wave vector k, a feature of backward MSSWs. The data of negative magnetic field (see supplementary materials) further prove the results of backward MSSWs.

To further substantiate our results, we compute the MSSW spectrum of Co/FeNi bilayer. The sample is schematically illustrated in the inset of Fig. 3(d). The sample is assumed to be infinite in xy-plane, and an magnetic field **H** is applied along x direction, the same as the experimental setup. The four regions denoted by $0 \sim 3$ are half-infinite vacuum, FeNi of thickness d_1, Co of thickness d_2, and half-infinite vacuum, respectively. For each region, the magnetostatic Maxwell's equations are[29,42]

$$\nabla \cdot \mathbf{B}_i = \mu_0 \nabla \cdot (\mathbf{H}_i + \mathbf{M}_i) = 0, \tag{1}$$

$$\nabla \times \mathbf{H}_i = 0, \tag{2}$$

where $|\mathbf{M}_i| = 0$ for vacuum $i = 0, 3$, $|\mathbf{M}_1| = M_{s,\mathrm{FeNi}}$, and $|\mathbf{M}_2| = M_{s,\mathrm{Co}}$. The Maxwell equation requires continuity of $\hat{\mathbf{z}} \times \mathbf{H}$ and $\hat{\mathbf{z}} \cdot \mathbf{B}$ at boundaries 01, 12, 23. The relationships between $\mathbf{H}_i$ and $\mathbf{M}_i$ in magnetic layers 1 and 2 come from Landau-Lifshitz-Gilbert (LLG) equation[43]

$$\frac{\partial \mathbf{M}_i}{\partial t} = -\gamma \mathbf{M}_i \times \left(\frac{A_i}{\mu_0 M_{si}^2} \nabla^2 \mathbf{M}_i + \mathbf{H}_i\right) + \frac{\alpha_i}{M_{si}} \mathbf{M}_i \times \frac{\partial \mathbf{M}_i}{\partial t}, \tag{3}$$

where A_i are the intralayer exchange constants in FeNi and Co, and α_i is the damping coefficient. If we do not consider surface effects such as surface anisotropy or surface spin transfer torque,[42] the LLG equation requires $\frac{\partial \mathbf{M}_i}{\partial z} = 0$ at boundaries 01 and 23, and the condition at boundary 12 is[44]

$$\frac{1}{2} \frac{A_{12}}{M_{s1} M_{s2}} (\mathbf{M}_{1+} \times \mathbf{M}_{2-}) + \frac{A_1}{M_{s1}^2} (\mathbf{M}_1 \times \frac{\partial \mathbf{M}_1}{\partial \mathrm{z}}) = 0 \tag{4}$$

$$\frac{1}{2} \frac{A_{12}}{M_{s1} M_{s2}} (\mathbf{M}_2 \times \mathbf{M}_1) + \frac{A_1}{M_{s2}^2} (\mathbf{M}_2 \times \frac{\partial \mathbf{M}_2}{\partial \mathrm{z}}) = 0 \tag{5}$$

where A_{12} is the interfacial exchange constant in units of J/m^2. We expand $\mathbf{M}_i$ and $\mathbf{H}_i$ around their equilibrium values,

$$\mathbf{M}_{1,2} = (M_{s1,2}, 0, 0) + \mathbf{m}_{1,2} \tag{6}$$

$$\mathbf{H}_i = (H, 0, 0) + \mathbf{h}_i \tag{7}$$

and keep only linear terms in the small quantities $\mathbf{m}_{1,2}$ and $\mathbf{h}_i$. By assuming a harmonic form $\mathbf{m}_{1,2}, \mathbf{h}_i \sim e^{i(\omega t - ky)}$ and applying the boundary conditions, we obtain a secular equation whose solution is the dispersion relation. The two lower frequency branches are MSSWs shown in Fig. 3 as the red dash curves that agree well with the experiment (bright green). The parameters are $M_{s1} = 0.77 \times 10^6$ A/m, $M_{s2} = 1.42 \times 10^6$ A/m, $\gamma = 28$ GHz/T, obtained from FMR experiments. The exchange constants as fitting parameters are $A_1 = 10$ pJ/m, $A_2 = 11$ pJ/m, and $A_{12} = 20$ mJ/m^2 that are reasonable. Indeed we also include the anisotropy field, see supplementary materials. The white dash lines in Fig. 3 indicates the PSSW frequency that decreases with the thickness of FeNi. Although the two layers are coupled, PSSWs can only be detected in the upper layer since the total thickness of bilayer is larger than the laser light penetration depth.

Figure 4 shows the theoretical group velocity as a function of positive wave vector with various model parameters. For different bilayer thicknesses, the phase velocities $v_p = \omega/k$ are always positive as shown in Fig. 3. While the group velocities $v_g = \partial\omega/\partial k$ are negative for most wave vector as shown in Fig. 4. For the FeNi layers of t = 30, 40, and 50 nm, group velocities change sign at the wave vector of $k_{\|}$ = 3.3, 2.45, and 1.95 rad/μm, respectively. The regions with opposite signs of phase velocities and group velocities are the backward SWs. It occurs when two magnetic layers have very different saturation

Copyright line will be provided by the publisher

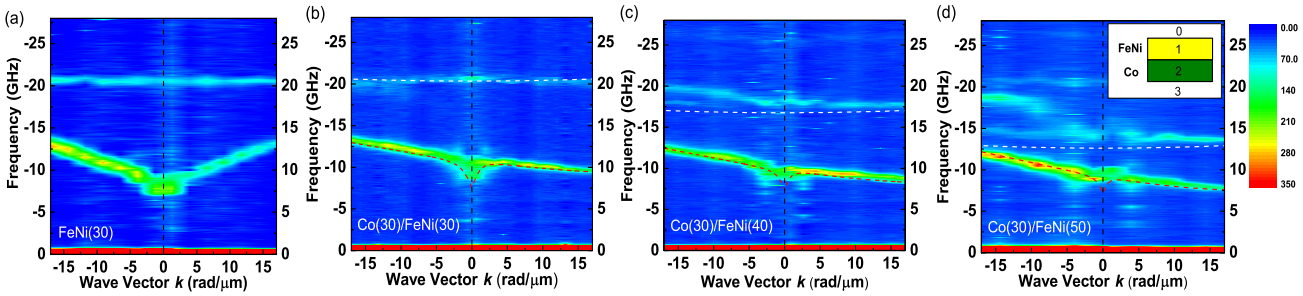

Figure 3 Density plot of BLS intensity in $\omega - k$ plane for FeNi(30) single layer (a) and Co/FeNi bilayer with various FeNi layer thicknesses of (b) t = 30 nm, (c) t = 40 nm, (d) t = 50 nm. The two sides of the vertical black dotted line correspond to different wave vector coordinates, respectively. The red dashed curves are of calculated MSSW spectrum. The white dashed curves are of the PSSW spectrum. The fixed external field $\mathbf{H} = 500$ Oe is applied along the x-direction. Inset: Schematic diagram of the bilayer system.

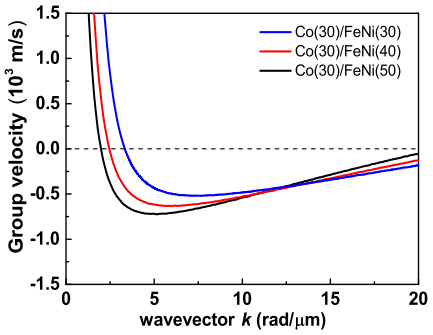

Figure 4 Theoretical calculations of group velocity as a function of positive wave vector for the different bilayer thicknesses.

magnetizations. It is the magnetostatic interaction between the two layers that leads to nonreciprocal behavior of SWs and the backward MSSWs.[28–32] The largest magnitudes of negative group velocities for FeNi layers of $t = 30$, 40, and 50 nm, are respectively 0.52, 0.64, and 0.72×10^3 m/s. It can be understood from the fact of increases of magnetostatic interaction and unchanged of the exchange interaction with the increases of layer thickness. As a result, the non-reciprocity becomes stronger [30], and, eventually, MSSWs become backward.

In summary, the backward MSSWs were observed in coupled Co/FeNi bilayer by BLS. The results were further confirmed by theoretical calculations. We revealed that coupling of two counter propagating MSSWs at the interface, through the magnetostatic interaction between two layers, is responsible for the BMSSWs. Furthermore, the largest magnitudes of negative group velocities increase with the thinkness of FeNi.

Supplementary material

The supplementary materials show several experimental measurements and detailed theoretical derivations for SWs. They include Part 1 for the ferromagnetic resonance(FMR) data and the relevant experimental parameters; Part 2 for the wave vector dependence of frequency at magnetic field **H** = -500 Oe; and Part 3 for the detailed derivation of spin wave spectrums.

Acknowledgements

This work is supported by the National Natural Science Foundation of China (NSFC) (Nos. 51871117, 51471080, 51671099, 11804045 and 61734002), the Program for Changjiang Scholars and Innovative Research Team in University (No. IRT-16R35), and the Fundamental of Research Funds for the Central Universities: lzujbky-2018-118.X.S.W. acknowledges the support from the Research Council of Norway through its Centres of Excellence funding scheme, Project No. 262633, “QuSpin”. X. R. W acknowledge supports from Hong Kong RGC (Grants No.16301518, 16301619 and 16300117).

References

[1] A. V. Chumak, V. I. Vasyuchka, A. A. Serga, and B. Hillebrands, Nat. Phys. **11**, 453 (2015).
[2] V. V. Kruglyak, S. O. Demokritov, and D. Grundler, J. Phys. D: Appl. Phys. **43**, 264001 (2010).
[3] A. A. Serga, A. V. Chumak, and B. Hillebrands, J. Phys. D: Appl. Phys. **43**, 264002 (2010).
[4] M. B. Jungfleisch, A. V. Chumak, V. I. Vasyuchka, A. A. Serga, B. Obry, H. Schultheiss, P. A. Beck, A. D. Karenowska, E. Saitoh, and B. Hillebrands, Appl. Phys. Lett. **99**, 182512 (2011).
[5] H. Ulrichs, V. E. Demidov, S. O. Demokritov, W. L. Lim, J. Melander, N. Ebrahim-Zadeh, and S. Urazhdin, Appl. Phys. Lett. **102**, 132402 (2013).
[6] A. V. Sadovnikov, E. N. Beginin, K. V. Bublikov, S. V. Grishin, S. E. Sheshukova, Y. P. Sharaevskii, and S. A. Nikitov, J. Appl. Phys. **118**, 203906 (2015).
[7] S. A. Odintsov, A. V. Sadovnikov, A. A. Grachev, E. N. Beginin, Y. P. Sharaevskii, and S. A. Nikitov, JETP Lett. **104**, 563 (2016).
[8] J. M. Owens, J. H. Collins, and R. L. Carter, Circuits Syst. Signal Process. **4**, 317 (1985).
[9] J. D. Adam, Proc. IEEE **76**, 159 (1988).
[10] A. V. Sadovnikov, S. A. Odintsov, E. N. Beginin, S. E. Sheshukova, Yu. P. Sharaevskii, and S. A. Nikitov, Phys. Rev. B **96**, 144428 (2017).

Copyright line will be provided by the publisher

[11] D. D. Stancil and A. Prabhakar,*Spin waves: Theory and applications* (New York: Springer), (2009).
[12] A. G. Gurevich and G. A. Melkov, *Magnetization Oscillations and Waves* (New York: CRC Press), (1996).
[13] R. W. Damon, and J. R. Eshbach, Phys. Chem. Solids. **19**, 308 (1961).
[14] R. W. Damon, and H. Van De Vaart, J. Appl. Phys. **36**, 3453 (1965).
[15] Y. S. Cao, P. Yan, H. Huebl, S. T. B. Goennenwein, and G. E. W. Bauer, Phy. Rev. B **91**, 094423 (2015).
[16] M. J. Hurben, and C. E. Patton, J. Magn. Magn. Mater. **139**, 263 (1995).
[17] D. D. Stancil, B. E. Henty, A. G. Cepni, and J. P. Van't Hof, Phys. Rev. B **74**, 060404 (2006).
[18] A. V. Chumak, P. Dhagat, A. Jander, A. A. Serga, and B. Hillebrands, Phys. Rev. B **81**, 140404 (2010).
[19] A. V. Sadovnikov, A. A. Grachev, S. E. Sheshukova, Y. P. Sharaevskii, A. A. Serdobintsev, D. M. Mitin, and S. A. Nikitov, Phys. Rev. Lett. **120**, 257203 (2018).
[20] V. E. Demidov, S. Urazhdin, A. Zholud, A. V. Sadovnikov, A. N. Slavin, and S. O. Demokritov, Sci. Rep. **5**, 8578 (2015).
[21] V. E. Demidov, S. Urazhdin, A. Zholud, A. V. Sadovnikov, and S. O. Demokritov, Appl. Phys. Lett. **105**, 172410 (2014).
[22] V. E. Demidov, S. Urazhdin, A. Zholud, A. V. Sadovnikov, and S. O. Demokritov, Appl. Phys. Lett. **106**, 022403 (2015).
[23] K. W. Reed, J. M. Owens, and R. L. Carter, Circuits Syst. Signal Process. **4**, 157 (1985).
[24] S. K. Kim, K. S. Lee, and D. S. Han, Appl. Phys. Lett. **95**, 082507 (2009).
[25] F. Garcia-Sanchez, P. Borys, R. Soucaille, J. P. Adam, R. L. Stamps, and J. V. Kim, Phys. Rev. Lett. **114**, 247206 (2015).
[26] X. S. Wang, H. W. Zhang, and X. R. Wang, Phys. Rev. Appl. **9**, 024029 (2018);
[27] X. S. Wang, Y Su, and X. R. Wang, Phys. Rev. B **95**, 014435 (2017).
[28] P. Grünberg, J. Appl. Phys. **52**, 6824 (1981).
[29] G. Rupp, W. Wettling, and W. Jantz, Appl. Phys. A **42**, 45 (1987).
[30] M. Mruczkiewicz, P. Graczyk, P. Lupo, A. Adeyeye, G. Gubbiotti, and M. Krawczyk, Phys. Rev. B **96**, 104411 (2017).
[31] J. L. Chen, T. Yu, C. P. Liu, T. Liu, M. Madami, K. Shen, J. Y. Zhang, S. Tu, M. S. Alam, K. Xia, M. Z. Wu, G. Gubbiotti, Y. M. Blanter, G. E. W. Bauer, and H. M. Yu, Phys. Rev. B **100**, 104427 (2019).
[32] R. A. Gallardo, T. Schneider, A. K. Chaurasiya, A. Oelschlägel, S. S. P. K. Arekapudi, A. Roldán-Molina, R. Hübner, K. Lenz, A. Barman, J. Fassbender, J. Lindner, O. Hellwig, and P. Landeros, Phys. Rev. Appl. **12**, 034012 (2019).
[33] A. V. Sadovnikov, E. N. Beginin, S. E. Sheshukova, Y. P. Sharaevskii, A. I. Stognij, N. N. Novitski, V. K. Sakharov, Y. V. Khivintsev, and S. A. Nikitov, Phys. Rev. B **99**, 054424 (2019).
[34] K. Di, V. L. Zhang, H. S. Lim, S. C. Ng, M. H. Kuok, J. W. Yu, J. Yoon, X. P. Qiu, and H. Yang, Phys. Rev. Lett. **114**, 047201 (2015).
[35] M. Belmeguenai, M. S. Gabor, Y. Roussigné, A. Stashkevich, S. M. Chérif, F. Zighem, and C. Tiusan, Phys. Rev. B **93**, 174407 (2016).
[36] H. Bouloussa, Y. Roussigné, M. Belmeguenai, A. Stashkevich, and S. M. Chérif, Phys. Rev. B **98**, 024428 (2018).
[37] W. F. Wang, G. Z. Chai, and D. S. Xue, J. Phys. D: Appl. Phys. **50**, 365003 (2017).
[38] S. O. Demokritov, B. Hillebrands, and A. N. Slavin, Phys. Rep. **348**, 441 (2001).
[39] C. W. Sandweg, M. B. Jungfleisch, V. I. Vasyuchka, A. A. Serga, P. Clausen, H. Schultheiss, B. Hillebrands, A. Kreisel, and P. Kopietz, Rev. Sci. Instrum. **81**, 073902 (2010).
[40] J. Jorzick, S. O. Demokritov, C. Mathieu, B. Hillebrands, B. Bartenlian, C. Chappert, F. Rousseaux, and A. N. Slavin, Phys. Rev. B **60**, 15194 (1999).
[41] D. Raasch, J. Reck, C. Mathieu, and B. Hillebrands,J. Appl Phys. **76**, 1145 (1994).
[42] J. Xiao and G. E. W. Bauer, Phys. Rev. Lett. **108**, 217204 (2012).
[43] T. L. Gilbert, IEEE. Trans. Magn. **40**, 3443 (2004).
[44] V. V. Kruglyak, O. Y. Gorobets, Y. I. Gorobets and A. N. Kuchko, J. Phys.: Cond. Matt. **26**, 406001 (2014).

Copyright line will be provided by the publisher

Graphical Table of Contents

GTOC image:

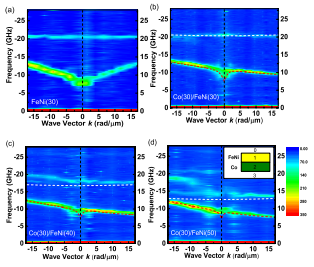

The dispersion relations of MSSWs obtained from the Stokes and anti-Stokes measurements display respectively positive and negative group velocities. The anti-Stokes branch with positive phase velocities and negative group velocities, known as backward magnetostatic surface mode originates from the magnetostatic interaction of the bilayer. Our results are useful for understanding the SWs propagation and miniaturizing SWs storage devices.

Copyright line will be provided by the publisher